



Cite this: *Chem. Sci.*, 2023, **14**, 2386

All publication charges for this article have been paid for by the Royal Society of Chemistry

Received 9th October 2022
Accepted 2nd January 2023

DOI: 10.1039/d2sc05600c
rsc.li/chemical-science

Introduction

Vancomycin is a critically important antibiotic, that was the drug of last resort against infections caused by multidrug-resistant Gram-positive bacteria.¹ It belongs to the glycopeptide class of antibiotics that consists of naturally occurring and semi-synthetic products that inhibit bacterial cell wall biosynthesis by binding to the D-Ala-D-Ala terminus of the cell wall precursor pentapeptide.^{1,2} However, widespread resistance to vancomycin that involves modification of the target peptide to D-Ala-D-Lac/D-Ser, concomitant with a reduction in binding affinity, and/or thickening of the cell wall has been reported.³ To incorporate additional mechanisms, second-generation glycopeptide antibiotics, telavancin, dalbavancin, and oritavancin, were equipped with lipophilic substitutions that abetted destabilization of the bacterial membranes.⁴ Despite reports of various modified glycopeptides that overcome inherited resistance,^{3,5–10} there are only a few reports of derivatives that

^aAntimicrobial Research Laboratory, New Chemistry Unit and School of Advanced Materials, Jawaharlal Nehru Centre for Advanced Scientific Research (JNCASR), Jakkur, Bengaluru, 560064, Karnataka, India. E-mail: jayanta@jncasr.ac.in; Tel: +91 802208 2565

^bDepartment of Life Sciences, School of Natural Sciences, Shiv Nadar University, Dadri 201314, UP, India

^cApplied Microbiology, Faculty of Biology and Biotechnology, Ruhr University Bochum, Universitätsstraße 150, 44780 Bochum, Germany

† Electronic supplementary information (ESI) available. See DOI: <https://doi.org/10.1039/d2sc05600c>

Next-generation membrane-active glycopeptide antibiotics that also inhibit bacterial cell division†

Paramita Sarkar,^a Kathakali De,^a Malvika Modi,^b Geetika Dhanda,^a Richa Priyadarshini, ^b Julia E. Bandow^c and Jayanta Haldar ^a

Resistance to vancomycin, a life-saving drug against Gram-positive bacterial infections necessitates developing alternative therapeutics. Herein, we report vancomycin derivatives that assimilate mechanisms beyond D-Ala-D-Ala binding. The role of hydrophobicity towards the structure and function of the membrane-active vancomycin showed that alkyl-cationic substitutions favored broad-spectrum activity. The lead molecule, VanQAmC₁₀ delocalized the cell division protein MinD in *Bacillus subtilis*, implying an impact on bacterial cell division. Further examination of wild-type, GFP-FtsZ, or GFP-FtsI producing- and Δ amiAC mutants of *Escherichia coli* revealed filamentous phenotypes and delocalization of the FtsI protein. The findings indicate that VanQAmC₁₀ also inhibits bacterial cell division, a property previously unknown for glycopeptide antibiotics. The conjunction of multiple mechanisms contributes to its superior efficacy against metabolically active and inactive bacteria, wherein vancomycin is ineffective. Additionally, VanQAmC₁₀ exhibits high efficacy against methicillin-resistant *Staphylococcus aureus* (MRSA) and *Acinetobacter baumannii* in mouse models of infection.

are effective against Gram-negative bacteria and dormant bacteria.^{11–15} The presence of an outer membrane in Gram-negative bacteria (GNB) precludes entry of numerous antibiotics including glycopeptides.¹⁶ Although the conjugation of membrane-interacting moieties onto glycopeptide antibiotics has shown activity against vancomycin-resistant Gram-positive bacteria, they do not necessarily result in activity against Gram-negative bacteria.¹⁷

We had developed C-terminally modified cationic lipophilic vancomycin derivatives that were effective against both vancomycin-resistant Gram-positive and the intrinsically resistant Gram-negative bacteria.^{18–20} Their broad-spectrum antibacterial activity was attributed to the incorporation of membrane-perturbation properties through the conjugation of lipophilic cationic moieties. In this report, we first examine the structure–activity relationship of alkyl and aryl moieties as hydrophobic substituents and identify the most selective compound. The effect of various hydrophobic group substitutions on membrane perturbing ability, the antibacterial activity of exponential growth, and quiescent bacteria was therefore examined to gain insights for better designs. Of most significance, here, a study of the effect of the lead compound on the membrane, cell division, and associated proteins was performed to better understand the modes of action of this new semisynthetic glycopeptide antibiotic. The protein localization and morphological changes were evaluated upon treatment of *B. subtilis* producing GFP-MinD protein, *E. coli* producing various GFP-tagged cell division proteins and an



amidase lacking mutant. Further, the potential of the lead compound as a preclinical candidate has been demonstrated in the murine thigh infection model against MRSA and chronic burn-wound infection against *A. baumannii*.

Results

Structure-activity relationship study

Design rationale. The second-generation glycopeptide antibiotics dalbavancin, oritavancin and possess hydrophobic moieties conjugated to the vancosamine sugar.^{21–23} These antibiotics display improved activity against vancomycin-resistant bacteria. However, they are not active against Gram-negative bacteria. We had previously reported that the attachment of cationic lipophilic moieties onto the C-terminus of vancomycin results in interaction with the negatively charged bacterial membrane.¹⁵ However, compounds with activity against both Gram-positive and Gram-negative bacteria were also slightly toxic. To address this, two sets of derivatives with C-terminus amido-alkyl-cationic (1–5) and aryl-cationic (6–10) substitutions were designed (Fig. 1A) and synthesized (Scheme S1†). The amphiphilicity of the cationic lipophilic moiety can be varied to selectively target the anionic bacterial membrane over the zwitterionic mammalian membrane. Biophysical studies and molecular dynamics simulation studies in polymeric and small molecular systems indicated that the inclusion of an amide spacer between the quaternary ammonium moiety and the hydrophobic moiety enhances the selectivity towards bacterial cells over mammalian cells.^{24,25} The inclusion of an amide bond contributes to additional hydrogen bonding capacity to the bacterial lipids.²⁶ It was, therefore, envisioned that lipophilic cationic vancomycin derivatives with an amide spacer could result in improved selectivity towards bacteria.

Activity against Gram-positive bacteria. The antibacterial activity of vancomycin derivatives was determined as the lowest concentration required to completely inhibit bacterial growth (minimum inhibitory concentration, MIC). Against MRSA, the aryl-substituted derivatives 1–5 showed activity similar to vancomycin (Table 1). The increase in the carbon content of substituted moieties from six (1) to seven (2 and 3) to ten (5) to twelve (4), increased activity. Among these derivatives, the biphenyl-substituted, VanQbiph (4) was the most effective. It showed a 22 to 88-fold increase in activity as compared to vancomycin against VRSA. Against VRE, it showed a 40- to 60-fold enhancement in activity.

Among the amido-alkyl substituted compounds, 6–8 exhibited MICs similar to that of vancomycin against MRSA while the longer chain variants, 9 and 10 showed reduced activity. Against VRSA, the lower chain length variants, 6 and 7 were less effective; VanQAmC₁₀ (8) showed a significant 115–490-fold improvement in activity as compared to vancomycin. 9 and 10 had similar MICs and were slightly more effective than 8. Against VRE, VanQAmC₁₀ (8) showed activity similar to that against VRSA (~160-fold improvement in activity as compared to vancomycin). In general, the series of amido-alkyl derivatives, 6–10 exhibited an increase in activity with longer chains, with no further enhancement in activity between longer chain

substituted derivatives 9 and 10. The amido-alkyl chain containing compounds exhibited better activity than those with aromatic substitutions. This indicated that the more flexible hydrophobic alkyl chain moieties resulted in better activity. VanQbiph (4), VanQAmC₁₀ (8), and VanQAmC₁₂ (9) demonstrate potency against vancomycin-resistant Gram-positive bacteria and were potential lead candidates. VanQAmC₁₀ shows activity similar to telavancin and is better than dalbavancin. The MIC of semi-synthetic glycopeptides such as oritavancin, telavancin and dalbavancin against VRE (VanA phenotype) were reported as 0.14 μM, 4 μM and 18 μM respectively.^{4,20,41}

Activity against Gram-negative bacteria. While the aromatic hydrophobicity containing compounds 1–5 did not show significant activity, the alkyl-containing derivatives (6–10) were active against *A. baumannii* (Table 1). The activity against *P. aeruginosa* was strain-dependent, and the compounds were inactive against *K. pneumoniae*. Against *A. baumannii* (MTCC 1425 and AB R674), 6 and 7 were moderately active, while 8–10 showed improved activity with an MIC value of 6.3 μM. Against an MDR strain of *P. aeruginosa* 8–10 exhibited the highest activity. In general, compounds with higher hydrophobicity, 8–10, displayed similar activity against Gram-negative bacteria. The results indicate that alkyl-cationic moieties are necessary for the antibacterial activity of vancomycin derivatives against Gram-negative bacteria. Of these, VanQAmC₁₀ (8) and VanQAmC₁₂ (9) demonstrated the highest activity against both Gram-positive and Gram-negative bacteria.

Hemolytic activity. To select the lead compounds, the toxicity of 1–10 was tested against human erythrocytes as their hemolytic activity (HC₅₀). The HC₅₀ is determined as the concentration at which 50% of the compound treated cells are lysed. The compounds with aromatic substitutions, 1–5, possessed lower antibacterial activity and were also non-toxic (Table 1). The HC₅₀ for compounds 6–8 was also greater than 500 μM. Compounds 9 and 10 with longer chain length caused hemolysis. Based on the *in vitro* activity and hemolysis studies, VanQbiph (4) from the aryl-substituted compounds and VanQAmC₁₀ (8) from the alkyl-chain substituted compounds were selected for further investigations. VanQAmC₁₀ (8) was found to be non-toxic to MDCK cells with CC₅₀ >64 μM (Fig. S1†). VanQAmC₁₀ (8) was additionally non-toxic to RAW 264.7 cells up to 40 μM and was therefore taken forward *in vivo* investigation.¹⁸

Eradication of exponentially growing bacteria

To examine the antibacterial properties of the two leads, VanQbiph (4) and VanQAmC₁₀ (8), the kinetics of bactericidal activity against exponentially growing, log-phase cells of MRSA was evaluated (Fig. 1B). The minimum bactericidal concentration (MBC) of VanQbiph (4) and VanQAmC₁₀ (8) was at 2×MIC. VanQAmC₁₀ (8) showed faster killing than both VanQbiph (4) and vancomycin. At 2×MIC, both the compounds exhibited complete eradication in 24 h like vancomycin. At 8×MIC, VanQAmC₁₀ (8) showed complete eradication within 6 h while VanQbiph (4) showed a similar effect at 24 h. VanQAmC₁₀ (8)



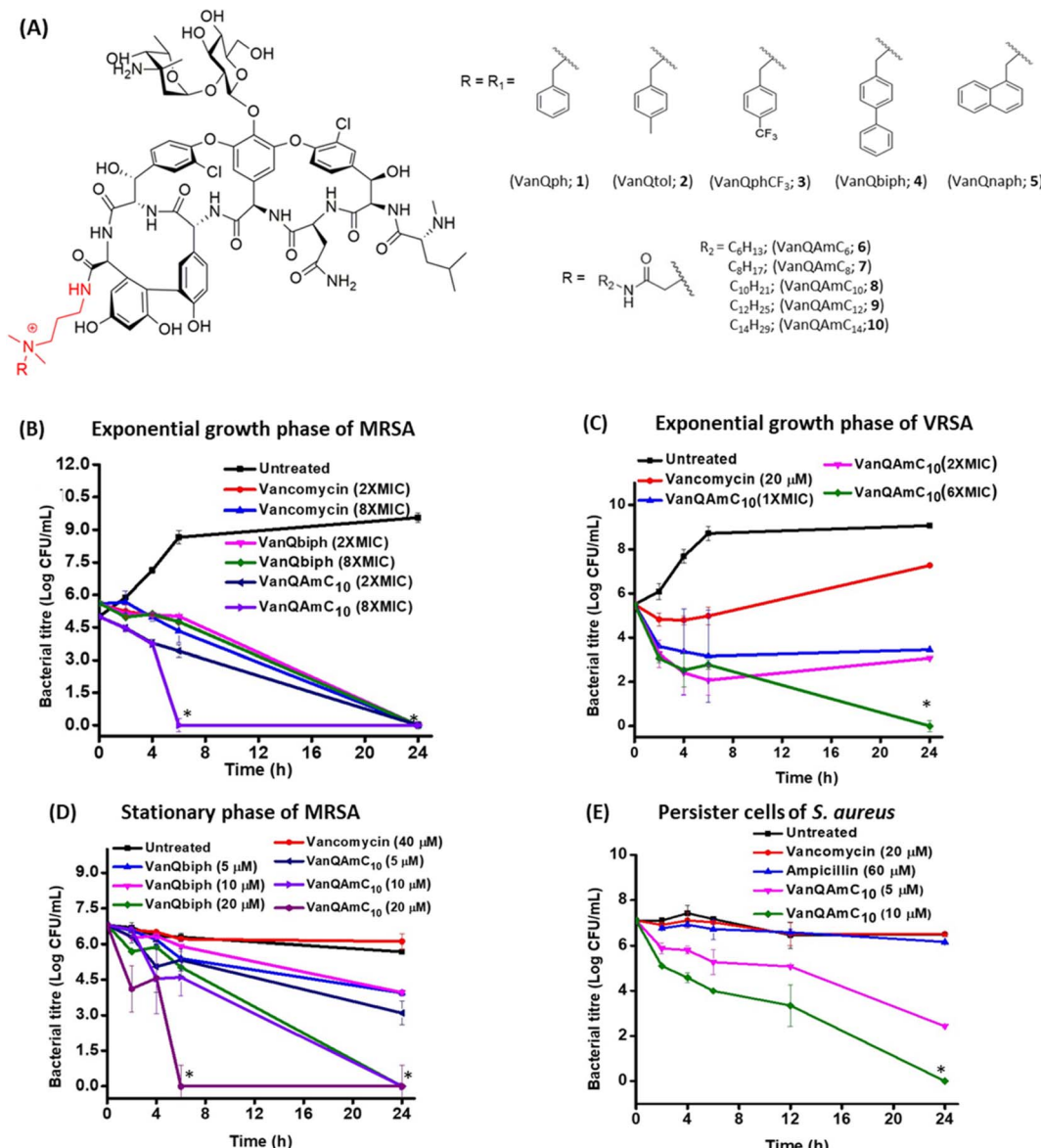


Fig. 1 (A) Structure of cationic lipophilic vancomycin derivatives. Bactericidal kinetics of (B) VanQbiph and VanQAmC₁₀ against exponential growth phase MRSA, (C) VanQAmC₁₀ against VRSA, (D) VanQbiph and VanQAmC₁₀ against stationary phase cells of MRSA, and (E) VanQAmC₁₀ against persister cells of *S. aureus*. Against MRSA, MIC of VanQAmC₁₀ = 0.4 µM, MIC of VanQbiph = 0.5 µM; MIC of VanQAmC₁₀ against VRSA = 1.6 µM and '*' indicates <50 CFU mL⁻¹.

showed a time and concentration-dependent activity while VanQbiph (**4**) and vancomycin showed only a time-dependent activity.

Against VRSA, VanQAmC₁₀ (**8**) exhibited better efficacy than VanQbiph (**4**) and was therefore tested for kinetics of killing. At MIC, it reduced the bacterial titer by 1.9 log CFU mL⁻¹ in 24 h (Fig. 1C). At 2×MIC, an initial reduction was observed, followed by a 1 log CFU mL⁻¹ increase in bacterial titer between 6 h and 24 h. At 6×MIC VanQAmC₁₀ resulted in complete eradication after 24 h. Treatment with vancomycin at 20 µM (sub-MIC), showed an initial growth inhibitory effect, followed by resumption of bacterial growth. Resistance in VRSA results from a combination of target modification as well as thickening of

the cell wall. The additional mechanisms of VanQAmC₁₀ possibly contribute to its bactericidal activity against VRSA.

Eradication of metabolically inactive bacteria

The stationary phase cells and persister cells are metabolically repressed and phenotypically different from the log-phase cells.²⁷ For activity, the commonly used drugs, vancomycin, and linezolid require actively ongoing cellular processes. They are therefore ineffective against non-dividing bacteria. Even at the concentration of 40 µM, vancomycin did not reduce the number of viable stationary phase cells of MRSA in 24 h (Fig. 1D). The integrity of the bacterial membrane is imperative to survival irrespective of metabolic state. VanQbiph (**4**) and

Table 1 Antibacterial activity and hemolysis of vancomycin derivatives (1–10) against multi-drug-resistant Gram-positive and Gram-negative bacteria^a

Compound	Minimum inhibitory concentration (μM)						Gram-negative bacteria			
	Gram-positive bacteria					Gram-negative bacteria				
	MRSA	VRSA 1	VRSA 4	VRSA 12	VRE 51575	VRE 51559	AB 1425	PA R590	AB R674	HC ₅₀ (μM)
Vancomycin	0.6	345	345	345	750	250	100	100	100	N.D
VanQph (1)	1	>30	>30	>30	>30	>30	>30	>30	25.5	>500
VanQtol (2)	1	>30	16	>30	>30	>30	>30	>30	25.3	>500
VanQphCF ₃ (3)	1	>30	15.8	>30	>30	>30	>30	24.6	24.6	>500
VanQbiph (4)	0.5	7.8	3.9	15.7	12.3	6.1	15.7	>30	24.5	>500
VanQnaph (5)	1	>30	3.9	>30	25	25	>30	>30	24.8	>500
VanQAmC ₆ (6)	0.8	>30	6.3	>30	>30	25	25	12.5	12.5	>500
VanQAmC ₈ (7)	0.8	3.1	3.1	>30	25	12.5	12.5	6.3	12.5	>500
VanQAmC ₁₀ (8)	0.4	3.1	1.6–3.1	1.6	4	4	6.3	3.1	10	>500
VanQAmC ₁₂ (9)	3.12	1.5	0.7	3	3.1	1.5	6.3	6.3	6.3	350
VanQAmC ₁₄ (10)	6.25	3	1.5	3	3.1	1.5	6.3	6.3	12.5	150

^a MRSA, methicillin-resistant *S. aureus* (ATCC 33591); VRSA, vancomycin-resistant *S. aureus*; VRE vancomycin-resistant *E. faecium* (VanA phenotype, ATCC 51559); vancomycin-resistant *E. faecalis* (VanB phenotype, ATCC 51575); ND, not determined. MIC against VRE and VRSA, HC₅₀ of VanQAmC₁₀ was previously reported.¹⁸

VanQAmC₁₀ (8) were designed to incorporate membrane activity and therefore expected to be effective against the metabolically inactive cells of MRSA. VanQAmC₁₀ (8) showed better activity than VanQbiph (4) at the same concentration, similar to that observed against log-phase cells of MRSA. Irrespective of treatment concentration, VanQbiph (4), exhibited slow killing with no significant reduction in viability up to 6 h. Complete eradication was observed at a higher concentration of 20 μM in 24 h. VanQAmC₁₀ (8) showed rapid bactericidal activity that increased with concentration. It completely eradicated cells in 24 h at 10 μM and within 6 h at 20 μM.

Persister cells are a subpopulation of bacterial cultures that are refractory to antibiotic treatment.²⁸ Since VanQAmC₁₀ (8) was more effective than VanQbiph (4) against stationary phase cultures, its activity against persister cells was evaluated. VanQAmC₁₀ (8) exhibited a concentration-dependent bactericidal activity against the persister cells of MRSA (Fig. 1D). This activity was more rapid than that observed against stationary phase cells.

Another growing challenge in treating bacterial infections is the formation of biofilms, which are recalcitrant to antibiotic treatment.²⁹ Most antibiotics including vancomycin are rendered ineffective against biofilms consisting of both dividing and non-dividing cells, majorly due to their inability to penetrate through the extracellular polymeric matrix. Thus, it is important to develop compounds that eradicate biofilms as well as planktonic cells. Untreated biofilms of MRSA grew to a thickness of 11.8 μm (Fig. S3A†). The vancomycin-treated biofilms remained intact with thickness similar to the untreated control. VanQAmC₁₀ (2) was found to reduce the thickness of biofilms of MRSA by about 40%, showing a thickness of 7.4 μm as opposed to 11.8 and 10.1 μm for untreated and vancomycin treated cases respectively (Fig. S3B and C†).

Mechanism of action against Gram-positive bacteria

Membrane depolarisation. Having established the superior antibacterial properties of cationic lipophilic vancomycin derivatives, their modes of action were probed. The membrane disruption properties of both VanQbiph (4) and VanQAmC₁₀ (8) were studied to correlate the extent of membrane perturbation and bactericidal activity against both exponentially growing and non-growing bacterial cells. Their ability to depolarize the membrane was monitored using the fluorescent probe DiSC₃(5) (3,3'-dipropylthiadicarbocyanine iodide). DiSC₃(5) is sensitive to the membrane potential and as it accumulates in the membrane, the fluorescence intensity decreases due to self-quenching. Upon dissipation of membrane potential, an increase in fluorescence is observed due to DiSC₃(5) being dispersed in the solution. Against *B. subtilis* and MRSA, both the compounds VanQbiph (4) and VanQAmC₁₀ (8) depolarised the membrane within 2 minutes post-treatment at 10 μM (Fig. 2A and B). The depolarization occurred in a concentration-dependent manner (Fig. S2A†). The alkyl chain substituted compound, VanQAmC₁₀ (8) showed a higher extent of depolarisation than the aromatic biphenyl substituted, VanQbiph (4). Against stationary phase cells of MRSA also, rapid dissipation of membrane potential was observed within 2 minutes post-treatment with both VanQbiph (4) and VanQAmC₁₀ (8) (Fig. 2C). Vancomycin did not affect the membrane potential.

Membrane permeabilization. The kinetics of permeabilization of membranes of MRSA and *B. subtilis* by the compounds was measured by the uptake of propidium iodide (PI). The dye, PI does not permeate through intact membranes. When the membrane integrity is compromised, it enters the cell and fluoresces upon binding to the DNA. Both VanQbiph (4) and VanQAmC₁₀ (8) permeabilized the membrane in a concentration-dependent manner (Fig. S2†). While vancomycin does not affect the membrane integrity, VanQAmC₁₀ (8) exhibited rapid permeabilization within 4 minutes of treatment. VanQbiph (4)

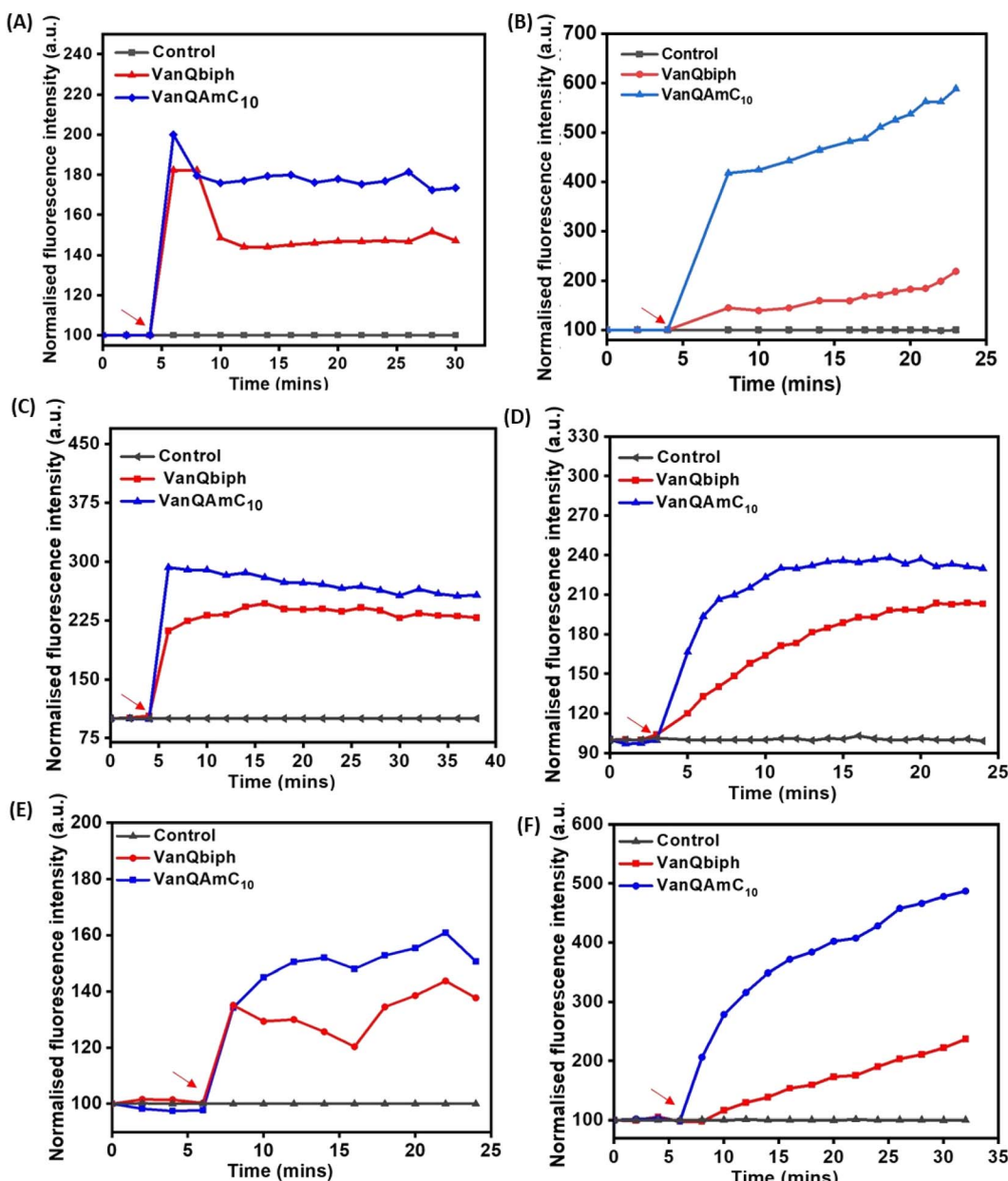


Fig. 2 Membrane–perturbation properties of VanQbiph and VanQAmC₁₀. Membrane depolarization against, (A) exponentially growing MRSA, (B) exponentially growing *B. subtilis*, upon treatment at 10 μ M, and (C) stationary phase cells of MRSA upon treatment at 20 μ M. Membrane permeabilization against, (D) exponentially growing MRSA, (E) exponentially growing *B. subtilis*, upon treatment at 10 μ M, and (F) stationary phase cells of MRSA upon treatment at 20 μ M. Red arrows indicate compound addition. The error percentage between replicates of an experiment was lesser than 5%. The images are representative of results from three independent experiments.

showed slower permeabilization (Fig. 2D and E). They caused gradual permeabilization against the stationary phase cells of MRSA as well (Fig. 2F). The extent of permeabilization was higher for VanQAmC₁₀ (8) than VanQbiph (4) against both the log-phase and stationary-phase bacteria similar to that observed during depolarisation. Membrane-perturbation may be the predominant mechanism leading to the antibacterial activity against metabolically inactive bacteria.

To confirm that membrane perturbation contributed to cell death, the bacterial viability was evaluated under conditions

similar to the mechanistic studies. A decrease in the number of viable cells was observed with an increase in the concentration of both VanQbiph (4) and VanQAmC₁₀ (8) (Fig. 3A). The number of viable cells was lower upon treatment with VanQAmC₁₀ (8) than when treated with VanQbiph (4) at the same concentration. At 5 μ M and 10 μ M, VanQbiph (4) showed 0.8 log CFU mL⁻¹ and 2.2 log CFU mL⁻¹ reduction respectively. VanQAmC₁₀ (8) showed 2 log CFU mL⁻¹ and 4 log CFU mL⁻¹ reduction upon treatment at 5 μ M and 10 μ M respectively. Treatment with both the compounds at 20 μ M resulted in complete eradication of the

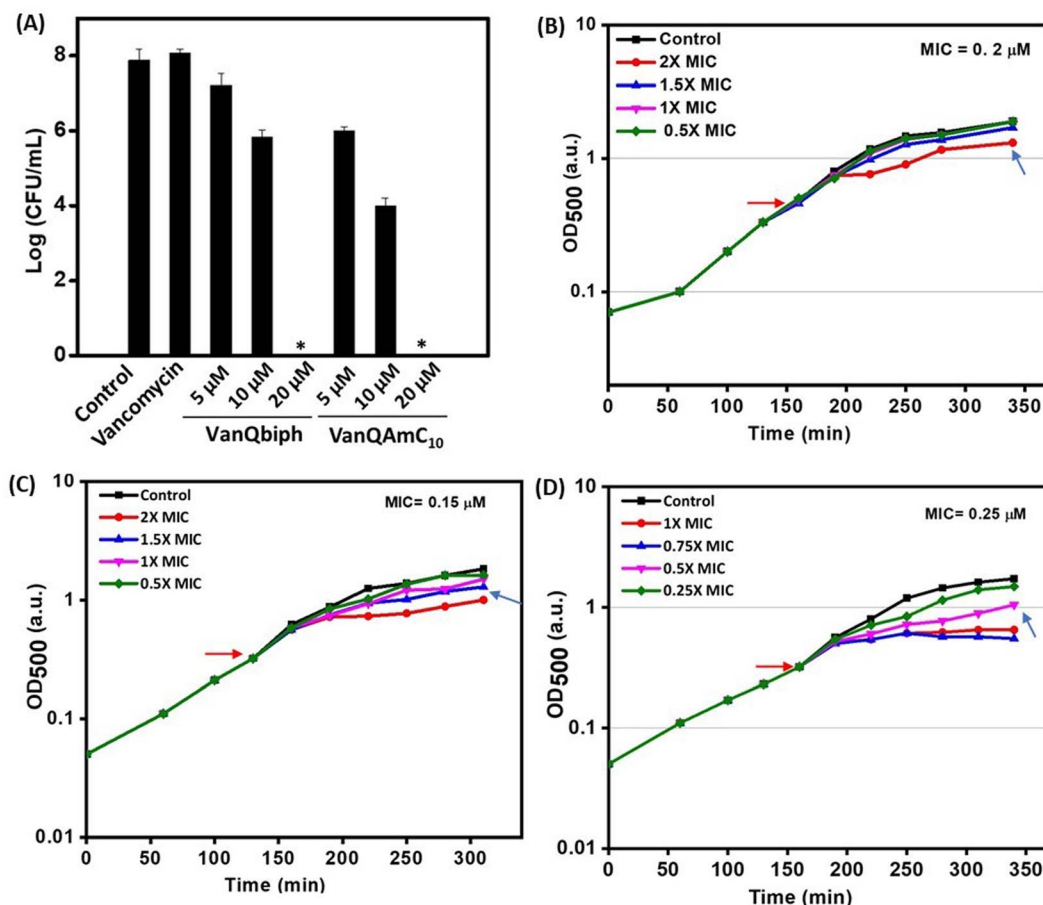


Fig. 3 (A) Viability of planktonic cells post-treatment in HEPES-glucose; acute growth retardation upon treatment with (B) vancomycin, (C) VanQbiph, (D) VanQAmC₁₀. '*' indicates <50 CFU mL⁻¹. Red arrow indicates compound addition and blue arrow indicates PEC.

bacteria. Vancomycin did not reduce the viability of bacteria even at 40 μM, under the same conditions. The stronger membrane-perturbation properties of VanQAmC₁₀ (8) therefore contribute to higher activity against both exponentially growing and stationary phase bacteria.

Acute effect on bacterial growth. The mechanisms of action in Gram-positive bacteria were further examined in the model bacterium *B. subtilis*. The study of the mechanism of action of a drug requires live cells under antibiotic stress. A 30–50% growth inhibition upon treatment, triggers a stress response in the bacterial cell while allowing cell proliferation to progress at a level sufficient to study the effect of the compound. The lowest concentration at which this effect was observed, was termed the physiologically effective concentration (PEC). The MIC of vancomycin, VanQbiph (4), and VanQAmC₁₀ (8) against *B. subtilis* were 0.2 μM, 0.15 μM, and 0.25 μM, respectively. The acute effect of different antibiotic concentrations on exponentially growing bacterial cultures were tested to identify the PEC (Fig. 3B–D). Vancomycin showed growth retardation at 0.4 μM. Similar growth retardation was observed at lower concentrations for both compounds. VanQAmC₁₀ (8) showed an inhibitory effect from 0.125 μM, while VanQbiph (4) showed a similar inhibition effect from 0.2 μM. The presence of cationic

lipophilic moieties possibly result in higher accumulation in the membrane region leading to growth inhibition at lower concentrations.

Cell wall biosynthesis inhibition. To further study the mechanisms contributing to the growth retardation, microscopic studies were carried out upon treatment of *B. subtilis* with compounds. Upon inhibition of cell wall biosynthesis, holes are formed in the peptidoglycan layer where new cell wall material is no longer incorporated. The cytoplasmic membrane extrudes out of these perforations, appearing as bubbles on the cell surface when treated with a 1 : 3 mixture of acetic acid and methanol.³⁰ This phenomenon is exhibited by compounds that inhibit cell wall biosyntheses like vancomycin and not agents that only perturb the membrane integrity such as gramicidin-A and valinomycin.³¹ Like vancomycin, VanQbiph (4) and VanQAmC₁₀ (8) showed bubbles on the surface, indicating that they inhibit cell wall biosynthesis and compromise the integrity of the cell wall (Fig. 4A).

MinD delocalization. MinD is a peripheral membrane protein that localizes at the cell poles and is part of the cell division regulation machinery. It has been reported that treatment with membrane-depolarizing agents like valinomycin results in the delocalization of the protein which appears in



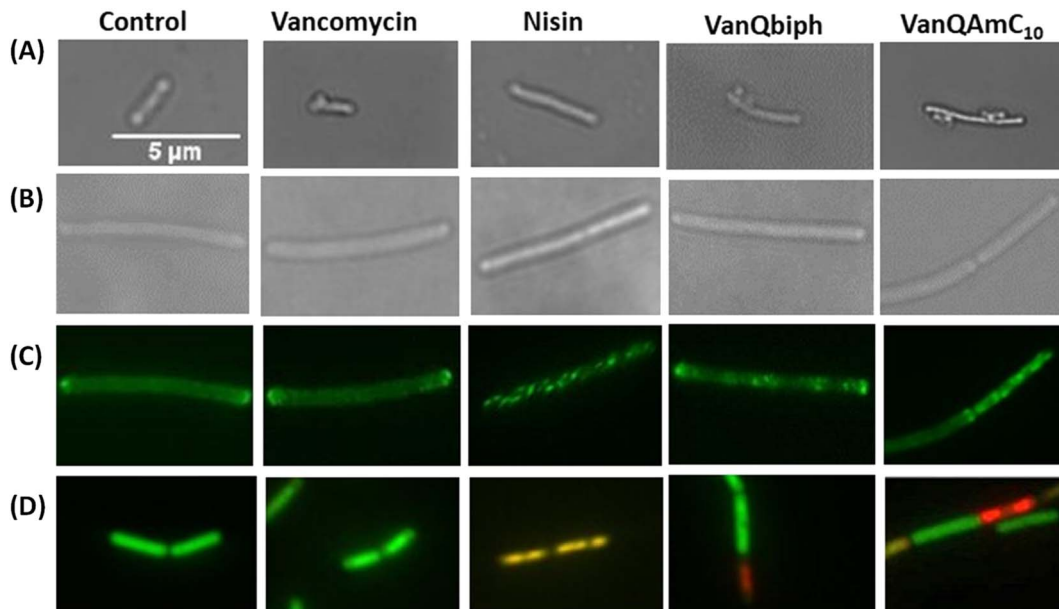


Fig. 4 Examination of the effect of VanQbiph, VanQAmC₁₀, vancomycin and nisin on cell membrane and wall integrity of *B. subtilis* upon treatment at respective PECs. (A) Inhibition of cell wall biosynthesis and compromise of cell wall integrity by visualization of 'bubbles' on the bacterial surface post acetic acid/methanol fixation through light microscopy; (B) light microscopy to assess the morphology of GFP-MinD expressing *B. subtilis* cells; (C) delocalization of GFP-MinD through fluorescence microscopy; (D) membrane permeabilization and pore formation monitored through fluorescence with the BacLight bacterial viability kit. Scale of all images is the same (5 μ m).

irregularly distributed spots throughout the cell. Since the compounds depolarise the bacterial membrane, their effect on the localization of the GFP-tagged MinD protein of *B. subtilis* was investigated. Treatment with VanQbiph (4) and VanQAmC₁₀ (8) at the PEC resulted in an irregular distribution of GFP-labelled MinD across the cells (Fig. 4B and C). This indicates that the compound also possibly stalls the bacterial cell division process.

Membrane permeabilization without pore formation. To examine if the compounds form pores on the membrane, a mixture of the fluorescent dyes SYTO 9 and PI was used. While SYTO 9 penetrates both intact and permeabilized cells staining them green, PI is unable to cross the intact membrane and stains only permeabilized or dead cells red. Membrane-disrupting antibiotics such as nisin are known to form pores in the membrane is stained by both SYTO 9 and PI (Fig. 4D). However, upon treatment with VanQbiph (4) and VanQAmC₁₀ (8), cells did not co-stain cells with both the dyes, indicating non-specific interaction with the membrane. Around 20% of the cells visualized post-treatment with both compounds were stained by PI and therefore permeabilized.

Antagonization assay with *N,N'*-diacetyl-*L*-Lys-*D*-Ala-*D*-Ala (Ac₂KAA) and teichoic acid. Ac₂KAA can act as a competitive ligand to the target of glycopeptide antibiotics and therefore antagonize antibacterial activity. In the presence of 500 μ M of Ac₂KAA, the activity of VanQAmC₁₀ (8) was reduced by 2-fold. However, the MIC of vancomycin increased from 0.6 μ M to >30 μ M (>40-fold increase in MIC) in presence of the same amount of Ac₂KAA. The 2-fold reduction in the activity of VanQAmC₁₀ (8) accounts for the loss of activity due to *D*-Ala-*D*-Ala binding. This

implied that it acted through additional mechanisms that are independent of *D*-Ala-*D*-Ala binding. The presence of the positive charge in VanQAmC₁₀ (8) could result in interactions with the negatively charged components of the bacterial cell wall like teichoic acid. C-terminal trimethyl ammonium modified vancomycin derivative has been reported to bind to teichoic acid.³² However, no change in the MIC of both vancomycin and VanQAmC₁₀ was observed in presence of lipoteichoic acid as a competing ligand, implying that it was not a target.

Mechanism of action in Gram-negative bacteria (*E. coli*)

Lysis of *E. coli*. The MIC of VanQAmC₁₀ (8) against *E. coli* was 16 μ M whereas vancomycin was inactive up to 66 μ M. Microscopic examination of *E. coli* treated with VanQAmC₁₀ at 25 μ M, showed that it completely lysed the cells, while vancomycin did not affect the cells (Fig. 5A). Over 240 minutes, *E. coli* treated with VanQAmC₁₀ (at 25 μ M), gradually grow bulky before finally lysing (ESI Video†). It punctured the cell, causing the cytoplasm to leak out as extrusions on the surface of the bacteria after which the cells flattened and disintegrated. Previous studies in Gram-negative bacteria indicated that VanQAmC₁₀ (8) can depolarise and permeabilize their outer and inner membrane.¹⁸

Effect on bacterial cell division. The division process broadly involves the following stages, (i) marking of the division site; (ii) employing the divisome and constriction of the cell wall through activation of cell wall synthesis; (iii) membrane fusion and cell wall hydrolysis for compartmentalization and physical separation into daughter cells.³³ It was envisioned that the membrane-perturbation properties of VanQAmC₁₀ (8) could affect bacterial cell division and the localization of associated



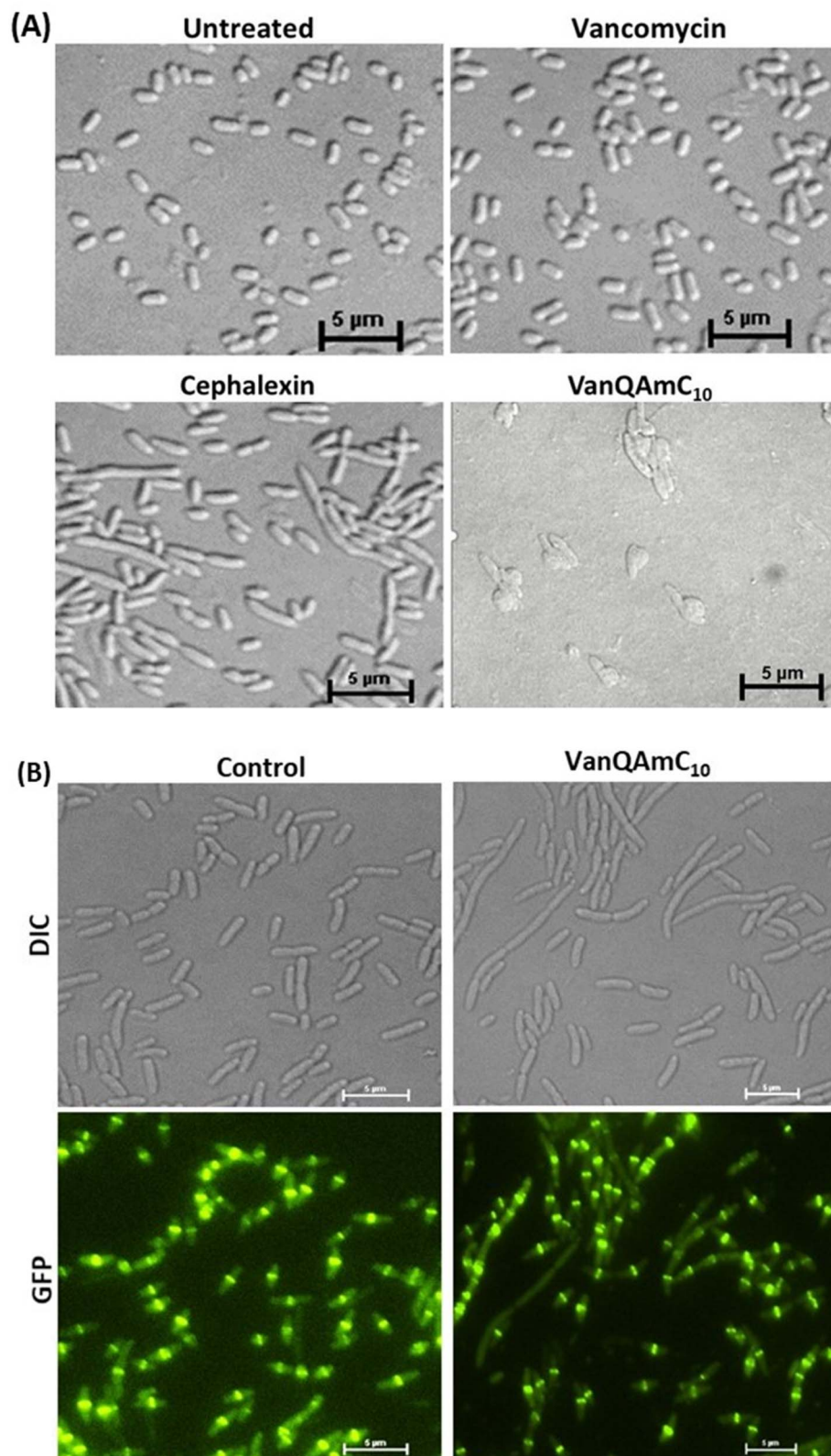


Fig. 5 Examination of *E. coli* cells treated with vancomycin, cephalexin and VanQAmC10 to study the effect on bacterial membrane integrity and cell division. (A) Light microscopy of wild-type *E. coli* upon treatment with vancomycin (34 μ M), and VanQAmC10 (25 μ M); (B) light and fluorescence microscopy in GFP-FtsZ expressing *E. coli* to assess morphological changes and localization of FtsZ post-treatment with VanQAmC10 (15 μ M) for 40 min; (C) delocalization of GFP-FtsZ in GFP-FtsZ expressing *E. coli* through fluorescence microscopy and morphological changes through light microscopy upon treatment with vancomycin (34 μ M), cephalexin (22 μ M) and VanQAmC10 (10 μ M); (D) light microscopy to assess morphological changes in *E. coli* MG1655 Δ amiAC mutant, when untreated and treated with vancomycin (3 μ M) and VanQAmC10 (2 μ M). Black arrows indicate morphological aberrations.



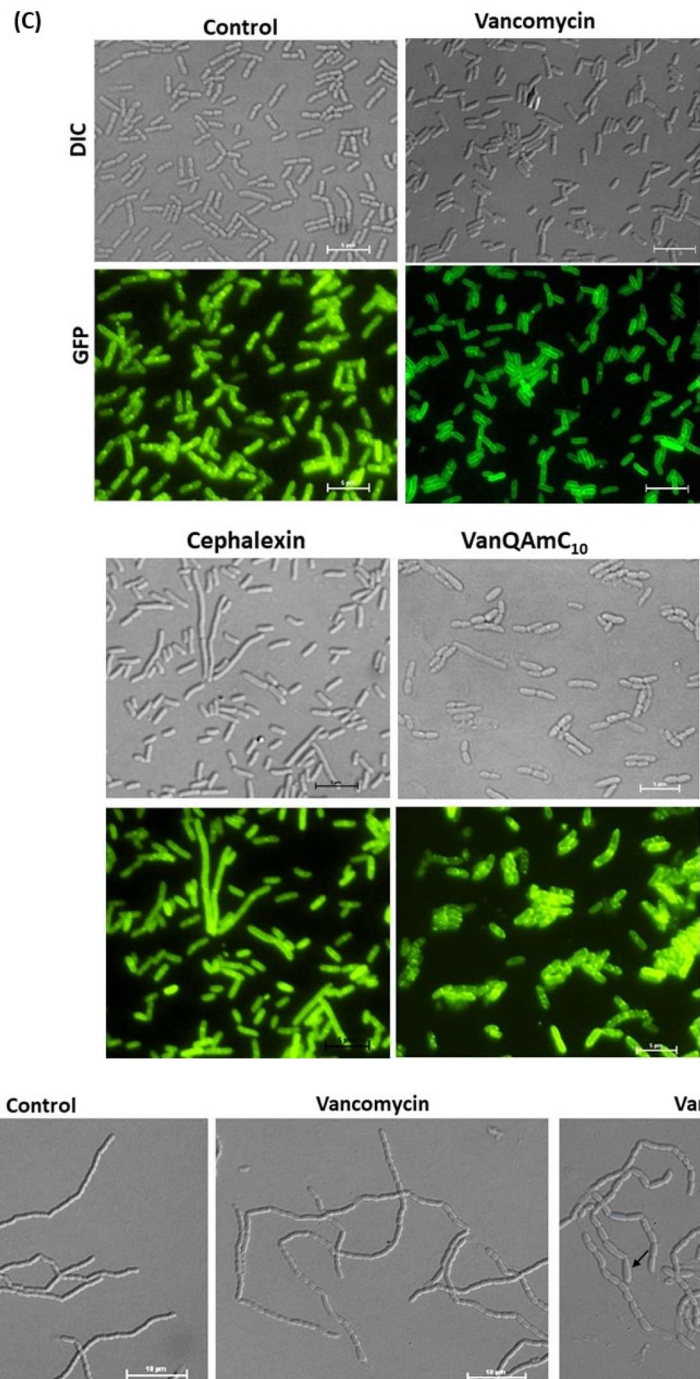


Fig. 5 (contd.)

proteins. Its effect on the various stages of cell division was investigated. In the first stage of cell division in bacteria, the particular localization of FtsZ at the septum is crucial. The effect of antibiotic treatment on localization and morphology against GFP-FtsZ producing bacteria was therefore first inspected.

Inhibition of cell division in GFP-FtsZ producing *E. coli*. The FtsZ protein assembles into a membrane-associated ring structure at the division septum. It recruits other proteins for the progression and completion of cell division.³⁴ The effect of

VanQAmC₁₀ on the localization of FtsZ and morphology in *E. coli* producing green fluorescent protein (GFP)-tagged FtsZ was studied through microscopy (Fig. 5B). The cells were treated with IPTG to overexpress *gfp-ftsZ* and then either treated with compounds or left untreated. Upon treatment with 15 μ M of VanQAmC₁₀, the cells appear to be filamentous with variable lengths of up to 4 μ m, while cells in the control group were \sim 2.5 μ m long. Incubation with VanQAmC₁₀ for a longer time (130 minutes) results in bulkier filamentous cells, with severely



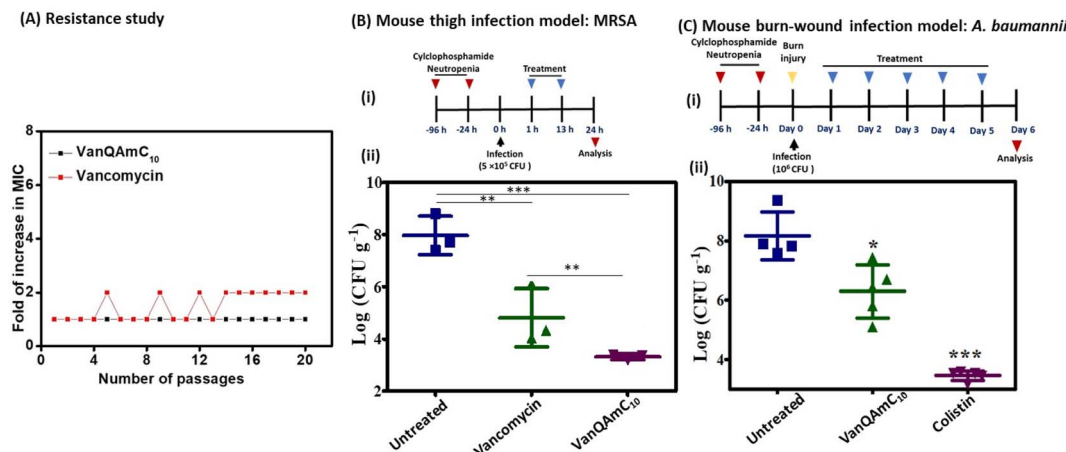


Fig. 6 (A) Propensity of vancomycin and VanQAmC₁₀ to induce resistance in MRSA upon serial exposure to sub-MIC concentrations; (B) (i) experimental design for *in vivo* efficacy study in a murine thigh infection model, (ii) *in vivo* efficacy of VanQAmC₁₀ and vancomycin against the multidrug-resistant methicillin-resistant *S. aureus* (MRSA) ($n = 3$ /dose). Antibiotics were administered intraperitoneally twice at 12 h intervals at a dose of 12 mg kg^{-1} . (C) (i) Experimental design for *in vivo* efficacy study in murine burn wound infection model, (ii) *in vivo* efficacy of VanQAmC₁₀ and colistin against the carbapenem-resistant *A. baumannii* ($n = 5$ /dose, 1 mouse died in untreated control). VanQAmC₁₀ and colistin were treated topically at 30 mg kg^{-1} for 5 days ('***' indicates $p < 0.0001$, '**' indicates $p < 0.001$, '*' $p < 0.05$, $p = 0.08$ (n.s.) for VanQAmC₁₀ with respect to vancomycin).

distorted shapes (Fig. S4†). However, the localization and distribution of Z-rings remain unaltered. IPTG-treated cells formed minicells of $\sim 1.5 \mu\text{m}$ length, which is characteristic of cells overproducing FtsZ.³⁵ Known inhibitors of FtsZ alter the regular midcell distribution of Z-rings.³⁶ The results indicate that VanQAmC₁₀ either affects FtsZ differently than the known inhibitors or that it inhibits bacterial cell division indirectly.

Mislocalization of GFP-FtsI protein. FtsI or PBP-3 is the only transpeptidase required for bacterial cell division and localizes to the septal ring.³⁷ It regulates the degree of cross-linking and coordinates the division process. GFP-tagged FtsI producing *E. coli* cells were treated with vancomycin (at $34 \mu\text{M}$) and VanQAmC₁₀ (at $10 \mu\text{M}$ and $15 \mu\text{M}$; Fig. 5C) and then examined under the microscope. The untreated and vancomycin-treated cells showed green fluorescence due to the localization of FtsI at the septum. Cephalexin, a known inhibitor of FtsI, induces a filamentous phenotype with mislocalized GFP-FtsI protein.³⁸ Upon treatment with $10 \mu\text{M}$ of VanQAmC₁₀, larger phenotypes of variable sizes are observed with shape defects. Some cells appear filamentous like in the case of cephalexin. The GFP-FtsI protein appears as green fluorescent spots delocalized across the cell in 60% of the cells visualized. At a higher concentration of $15 \mu\text{M}$, bulkier cells with more distorted shapes than those at $10 \mu\text{M}$ were observed (Fig. S5†). Thus, VanQAmC₁₀ mislocalizes the cell division protein, FtsI, and inhibits further cell division.

Sensitivity against mutants lacking AmiA and AmiC. The bacterial amidases help cleave the septum in the final stage of cell division to produce daughter cells.³⁹ In the absence of amidases, chains of unseparated cells are formed (Fig. 5D). These retain distinct cytoplasmic compartments but share an outer membrane.³⁹ These cells are known to be hypersensitive to antibiotics and detergents. However, ΔamiAC mutations are resistant to killing by cephalexin.³⁸ The MIC of VanQAmC₁₀ against the ΔamiAC mutant was reduced to $4 \mu\text{M}$, while that of

vancomycin was $>10 \mu\text{M}$. This indicates that VanQAmC₁₀ inhibits cell division through mechanisms different from cephalexin. Microscopic examination of the mutants treated with sub-inhibitory concentrations of VanQAmC₁₀ revealed larger cell phenotypes of variable sizes. This is indicative of impaired cell division. Cell debris due to lysis after compound treatment are also visible. In the vancomycin-treated cells, few cells appear larger and bulky while most appear similar to the untreated bacteria (Fig. 5D).

In vivo activity of VanQAmC₁₀

Resistance induction. Having observed the multiple mechanisms of VanQAmC₁₀, the potential as a preclinical candidate was examined. The multimodal mechanisms possibly lead to the lack of resistance development to VanQAmC₁₀ in MRSA after 20 passages, while vancomycin showed a 2-fold increase in MIC (Fig. 6A). Additionally, VanQAmC₁₀ does not induce resistance in *A. baumannii*, unlike colistin.¹⁸ The frequency of resistance for both vancomycin and VanQAmC₁₀ against MRSA was $<10^{-8}$ indicating the absence of spontaneous mutants.

Activity in mouse liver homogenate and human plasma. The MIC of VanQAmC₁₀ against MRSA and VRE remained unchanged in both plasma as well as liver homogenate, thereby confirming their stability for activity *in vivo* (Table S1†).

Efficacy in mouse infection models. The LD₅₀ of VanQAmC₁₀ (8) was found to be 70 mg kg^{-1} through intravenous injection.¹⁸ When administered intraperitoneally, a 130 mg kg^{-1} dose was found to be well tolerated and all mice survived. The LD₅₀ of VanQAmC₁₀ was greater than 160 mg kg^{-1} when administered subcutaneously. The *in vitro* activity, low toxicity, and stability in plasma and liver homogenate, supported the potential of VanQAmC₁₀ as a candidate for the treatment of bacterial infections. The efficacy of VanQAmC₁₀ (8) against MRSA was

tested in a neutropenic mouse thigh infection model. Infection was established by injecting them with 5×10^5 CFU of MRSA in the thigh. 1 h and 13 h post-infection, mice were treated with 12 mg kg⁻¹ of vancomycin and VanQAmC₁₀ administered intraperitoneally (Fig. 6B). The mice were sacrificed 24 h post-infection. The pre-treatment bacterial load was found to be 6.3 log CFU mL⁻¹. In the untreated group, the bacterial load increased to 8 log CFU g⁻¹. The vancomycin treated group showed a bacterial load of 4.8 log CFU g⁻¹ of tissue. However, treatment with VanQAmC₁₀ reduced the bacterial load to 3.3 log CFU g⁻¹, which is a 1.5 log CFU g⁻¹ lower bacterial load than observed against vancomycin. The results highlight the superior *in vivo* efficacy of VanQAmC₁₀ as compared to that of the parent drug vancomycin.

Further, the efficacy of VanQAmC₁₀ (8) was tested in a chronic burn-wound infection model of *A. baumannii*.⁴⁰ Chronic burn wounds on the back of mice were infected with *A. baumannii*. 24 h post-infection, before initiation of treatment, the bacterial load was found to be 7.5 log CFU g⁻¹. Infected mice were treated with 30 mg kg⁻¹ of VanQAmC₁₀ and colistin for five days consecutively. The bacterial load in the untreated group increased to 8 log CFU g⁻¹ six days post-infection. Treatment with VanQAmC₁₀ resulted in a 2.2 log CFU g⁻¹ lower bacterial load as compared to the untreated mice, while colistin showed a 4.8 log CFU g⁻¹ load lower bacterial load as compared to the untreated mice at the same dose (Fig. 6C). The use of colistin is however limited due to its toxicity and bacteria easily develop resistance to it. Therefore, VanQAmC₁₀ presents a promising alternative for both Gram-positive and Gram-negative bacteria.

Discussion

Vancomycin served as a life-saving drug against MDR Gram-positive bacterial infections for over thirty years until the report of resistance. This makes it an attractive drug for further development against the escalating incidences of resistant bacteria. The more difficult to treat Gram-negative bacteria are inherently resistant to vancomycin. We have shown that the conjugation of cationic lipophilic moieties to vancomycin results in broad-spectrum activity against both Gram-negative bacteria and Gram-positive bacteria. The cationic lipophilic moiety incorporates interaction with the negatively charged bacterial membrane, therefore, perturbing membrane integrity. Through comparison of alkyl and aryl-substituted derivatives, VanQAmC₁₀ and VanQbiph respectively, we demonstrate that the alkyl substitutions exhibit better membrane activity as well as bactericidal activity against both metabolically active and inactive bacteria (Fig. 1). Vancomycin, on the other hand, is ineffective against the metabolically inactive bacterial cells. The lead compound, VanQAmC₁₀ shows remarkable improvement in antibacterial efficacy in a mouse thigh infection model as compared to vancomycin against MRSA (Fig. 6). It was also effective against burn wound infections in mice caused by *A. baumannii*.

Scientific interest toward membrane-active vancomycin derivatives has been growing due to their ability to overcome both inherited and non-inherited resistance.³ Therefore,

a holistic understanding of how membrane-active vancomycin derivatives affect the bacteria would be imperative for the further development of new agents. In a step toward this, we used a variety of biological assays to provide new insights into the mechanism of action of VanQAmC₁₀. It acts through mechanisms in addition to cell wall synthesis inhibition by binding to the D-Ala-D-Ala terminus which is known for the parent drug, vancomycin. To rule out the secondary effects as a result of cell death, mechanisms of action were studied at sub-inhibitory concentrations. Systematic investigations in *B. subtilis* revealed that it acts by simultaneously, (i) inhibiting cell wall biosynthesis, (ii) permeabilizing cells through non-specific interactions with membrane, and (iii) dissipation of membrane-potential leading to delocalization of the cell division protein, MinD (Fig. 4). The dissipation of membrane potential by VanQAmC₁₀ possibly results in malfunctioning of the bacterial cell division machinery.⁴² To comprehend how VanQAmC₁₀ affects Gram-negative bacteria, studies were conducted on the model Gram-negative bacterium, *E. coli*. Treatment with VanQAmC₁₀ results in the lysis of the cells and therefore cell death. Treatment of the various strains of *E. coli* (wild-type, GFP-FtsI, GFP-FtsZ, and Δ amiAC) at subinhibitory concentrations resulted in cells of variable sizes and distorted morphology (Fig. 5). It did not impede the formation of the Z-ring in the first stage of cell division. It delocalized the FtsI protein required for the synthesis of the cell wall during septum formation in the second stage of cell division. Mutants lacking AmiA and AmiC enzymes were more sensitive to VanQAmC₁₀ which is consistent with reports that these mutants have increased susceptibility to surfactants. These confirm that VanQAmC₁₀ inhibits cell division at sub-inhibitory concentrations through mechanisms different from the FtsZ inhibitors and the β -lactam, cephalexin. Our findings suggest that the membrane perturbing properties of VanQAmC₁₀ affect the localization of proteins involved in cell division, leading to severe cell wall and membrane defects. This possibly ultimately leads to a breach in the cell membrane and cell death.

Overall, here we demonstrate a new vancomycin derivative, VanQAmC₁₀ which is highly effective against Gram-positive as well as Gram-negative bacteria both *in vitro* and *in vivo*. The multiple mechanisms of action contribute to the negligible resistance induction and superior antibacterial properties of VanQAmC₁₀ as compared to the parent drug. It represents a new class of multi-target, multi-effect glycopeptide antibiotics. The findings augment a new dimension to the understanding of the mechanism of such membrane-active glycopeptide derivatives.

Data availability

The datasets supporting this article have been uploaded as part of the ESI. The ESI† includes materials and methods; experimental protocols for *in vitro* microbiological assays (activity, biofilms, time-kill kinetics, and mechanistic studies) and toxicity, and *in vivo* activity and toxicity; supplementary figures; details of characterization of intermediates and final compounds through ¹H NMR, IR, and HR-MS.



Author contributions

PS, project design, synthesis, characterisation, performing *in vitro* microbiological assays (activity and mechanistic studies) and *in vivo* infection studies, data curation, formal analysis, manuscript writing and editing; KD, synthesis and characterisation; GD, cytotoxicity testing and *in vivo* activity studies, manuscript editing; JEB, experimental design and analysis for mechanisms of action against *B. subtilis*, manuscript editing; MM and RP, experimental design and analysis for mechanisms of action against *E. coli*, manuscript editing; JH, project design, research supervision, manuscript writing and editing.

Conflicts of interest

There are no conflicts to declare.

Acknowledgements

We acknowledge DST-DAAD bilateral cooperation project (INT/FRG/DAAD/P-15/2018) and JNCASR for funding. We thank Dr Sandip Samaddar (JNCASR), Dr Riya Mukherjee (JNCASR) and Pascal Dietze (RUB) for excellent technical support and scientific discussions. We thank Dr Chandradhish Ghosh and Dr Venkateswarlu Yarlagadda for fruitful scientific discussions. RP acknowledges funding from CSIR (37(1701)/17/EMR-II) and Shiv Nadar University. MM acknowledges support by DST Inspire fellowship. JEB acknowledges funding from the DAAD Program DST 2018 (57389759). We thank Dr Sidharth Chopra (Central Drug Research Institute, Lucknow) for the gift of drug-resistant clinical isolates.

References

- 1 <https://www.who.int/foodsafety/cia/en/>, 2019.
- 2 E. Binda, F. Marinelli and G. L. Marcone, *Antibiotics*, 2014, **3**, 572–594.
- 3 G. Dhanda, P. Sarkar, S. Samaddar and J. Haldar, *J. Med. Chem.*, 2019, **62**, 3184–3205.
- 4 D. Zeng, D. Debabov, T. L. Hartsell, R. J. Cano, S. Adams, J. A. Schuyler, R. McMillan and J. L. Pace, *Cold Spring Harb. Perspect. Med.*, 2016, **6**, a026989.
- 5 M. A. T. Blaskovich, K. A. Hansford, M. S. Butler, Z. Jia, A. E. Mark and M. A. Cooper, *ACS Infect. Dis.*, 2018, **4**, 715–735.
- 6 A. Okano, N. A. Isley and D. L. Boger, *Proc. Natl. Acad. Sci. U. S. A.*, 2017, **114**, E5052–E5061.
- 7 V. Yarlagadda, P. Sarkar, G. B. Manjunath and J. Haldar, *Bioorg. Med. Chem. Lett.*, 2015, **25**, 5477–5480.
- 8 V. Yarlagadda, P. Sarkar, S. Samaddar and J. Haldar, *Angew. Chem., Int. Ed. Engl.*, 2016, **55**, 7836–7840.
- 9 D. Guan, F. Chen, Y. Qiu, B. Jiang, L. Gong, L. Lan and W. Huang, *Angew. Chem., Int. Ed. Engl.*, 2019, **58**, 6678–6682.
- 10 A. Antonoplis, X. Zang, M. A. Huttner, K. K. L. Chong, Y. B. Lee, J. Y. Co, M. R. Amieva, K. A. Kline, P. A. Wender and L. Cegelski, *J. Am. Chem. Soc.*, 2018, **140**, 16140–16151.
- 11 M. M. Fernandes, K. Ivanova, J. Hoyo, S. Perez-Rafael, A. Francesko and T. Tzanov, *ACS Appl. Mater. Interfaces*, 2017, **9**, 15022–15030.
- 12 V. Yarlagadda, P. Sarkar, S. Samaddar, G. B. Manjunath, S. D. Mitra, K. Paramanandham, B. R. Shome and J. Haldar, *ACS Infect. Dis.*, 2018, **4**, 1093–1101.
- 13 A. Antonoplis, X. Zang, T. Wegner, P. A. Wender and L. Cegelski, *ACS Chem. Biol.*, 2019, **14**, 2065–2070.
- 14 E. van Groesen, C. J. Slingerland, P. Innocenti, M. Mihajlovic, R. Masereeuw and N. I. Martin, *ACS Infect. Dis.*, 2021, **7**, 2746–2754.
- 15 E. Lei, H. Tao, S. Jiao, A. Yang, Y. Zhou, M. Wang, K. Wen, Y. Wang, Z. Chen, X. Chen, J. Song, C. Zhou, W. Huang, L. Xu, D. Guan, C. Tan, H. Liu, Q. Cai, K. Zhou, J. Modica, S. Y. Huang, W. Huang and X. Feng, *J. Am. Chem. Soc.*, 2022, **144**, 10622–10639.
- 16 R. E. Impey, D. A. Hawkins, J. M. Sutton and T. P. Soares da Costa, *Antibiotics*, 2020, **9**.
- 17 M. A. T. Blaskovich, K. A. Hansford, Y. Gong, M. S. Butler, C. Muldoon, J. X. Huang, S. Ramu, A. B. Silva, M. Cheng, A. M. Kavanagh, Z. Ziora, R. Premraj, F. Lindahl, T. A. Bradford, J. C. Lee, T. Karoli, R. Pelington, D. J. Edwards, M. Amado, A. G. Elliott, W. Phetsang, N. H. Daud, J. E. Deecke, H. E. Sidjabat, S. Ramaolaga, J. Zuegg, J. R. Betley, A. P. G. Beevers, R. A. G. Smith, J. A. Roberts, D. L. Paterson and M. A. Cooper, *Nat. Commun.*, 2018, **9**, 22.
- 18 P. Sarkar, S. Samaddar, V. Ammanathan, V. Yarlagadda, C. Ghosh, M. Shukla, G. Kaul, R. Manjithaya, S. Chopra and J. Haldar, *ACS Chem. Biol.*, 2020, **15**, 884–889.
- 19 V. Yarlagadda, G. B. Manjunath, P. Sarkar, P. Akkapeddi, K. Paramanandham, B. R. Shome, R. Ravikumar and J. Haldar, *ACS Infect. Dis.*, 2016, **2**, 132–139.
- 20 V. Yarlagadda, P. Akkapeddi, G. B. Manjunath and J. Haldar, *J. Med. Chem.*, 2014, **57**, 4558–4568.
- 21 J. A. Karlowsky, K. Nichol and G. G. Zhan, *Clin. Infect. Dis.*, 2015, **61**(Suppl 2), S58–S68.
- 22 M. T. Guskey and B. T. Tsuji, *Pharmacotherapy*, 2010, **30**, 80–94.
- 23 G. G. Zhan, D. Calic, F. Schweizer, S. Zelenitsky, H. Adam, P. R. Lagace-Wiens, E. Rubinstein, A. S. Gin, D. J. Hoban and J. A. Karlowsky, *Drugs*, 2010, **70**, 859–886.
- 24 D. S. Uppu, P. Akkapeddi, G. B. Manjunath, V. Yarlagadda, J. Hoque and J. Haldar, *Chem. Comm.*, 2013, **49**, 9389–9391.
- 25 J. Hoque, S. Gonuguntla, V. Yarlagadda, V. K. Aswal and J. Haldar, *Phys. Chem. Chem. Phys.*, 2014, **16**, 11279–11288.
- 26 D. S. S. M. Uppu, M. M. Konai, U. Baul, P. Singh, T. K. Siersma, S. Samaddar, S. Vemparala, L. W. Hamoen, C. Narayana and J. Haldar, *Chem. Sci.*, 2016, **7**, 4613–4623.
- 27 X. Zhou and L. Cegelski, *Biochemistry*, 2012, **51**, 8143–8153.
- 28 I. Keren, N. Kaldalu, A. Spoerling, Y. Wang and K. Lewis, *FEMS Microbiol. Lett.*, 2004, **230**, 13–18.
- 29 D. E. Moormeier and K. W. Bayles, *Mol. Microbiol.*, 2017, **104**, 365–376.
- 30 T. Schneider, T. Kruse, R. Wimmer, I. Wiedemann, V. Sass, U. Pag, A. Jansen, A. K. Nielsen, P. H. Mygind, D. S. Raventos, S. Neve, B. Ravn, A. M. Bonvin, L. De



Maria, A. S. Andersen, L. K. Gammelgaard, H. G. Sahl and H. H. Kristensen, *Science*, 2010, **328**, 1168–1172.

31 M. Wenzel, B. Kohl, D. Munch, N. Raatschen, H. B. Albada, L. Hamoen, N. Metzler-Nolte, H. G. Sahl and J. E. Bandow, *Antimicrob. Agents Chemother.*, 2012, **56**, 5749–5757.

32 Z. C. Wu, N. A. Isley, A. Okano, W. J. Weiss and D. L. Boger, *J. Org. Chem.*, 2020, **85**, 1365–1375.

33 L. I. Rothfield and S. S. Justice, *Cell*, 1997, **88**, 581–584.

34 W. Margolin, *Nat. Rev. Mol. Cell Biol.*, 2005, **6**, 862–871.

35 J. E. Ward Jr and J. Lutkenhaus, *Cell*, 1985, **42**, 941–949.

36 L. Araujo-Bazan, L. B. Ruiz-Avila, D. Andreu, S. Huecas and J. M. Andreu, *Front. Microbiol.*, 2016, **7**, 1558.

37 M. C. Wissel and D. S. Weiss, *J. Bacteriol.*, 2004, **186**, 490–502.

38 H. S. Chung, Z. Yao, N. W. Goehring, R. Kishony, J. Beckwith and D. Kahne, *Proc. Natl. Acad. Sci. U. S. A.*, 2009, **106**, 21872–21877.

39 R. Priyadarshini, M. A. de Pedro and K. D. Young, *J. Bacteriol.*, 2007, **189**, 5334–5347.

40 M. G. Thompson, C. C. Black, R. L. Pavlicek, C. L. Honnold, M. C. Wise, Y. A. Alamneh, J. K. Moon, J. L. Kessler, Y. Si, R. Williams, S. Yildirim, B. C. Kirkup Jr, R. K. Green, E. R. Hall, T. J. Palys and D. V. Zurawski, *Antimicrob. Agents Chemother.*, 2014, **58**, 1332–1342.

41 J. M. Streit, *Diagn. Microbiol. Infect. Dis.*, 2004, **48**, 137–143.

42 P. Sarkar, *J. Med. Chem.*, 2021, 10185.

